

# Status of Pulsed Neutron Facility in Korea

Guinyun Kim<sup>a</sup>, Manwoo Lee<sup>a</sup>, Kyung Sook Kim<sup>a</sup>, Sungchul Yang<sup>a</sup>, Eunae Kim<sup>b</sup>, Valery Shvetshov<sup>b</sup>, Vadim Skoy<sup>b</sup>, Moo-Hyun Cho<sup>b</sup>, and Won Namkung<sup>c</sup>

<sup>a</sup>*Department of Physics, Kyungpook National University, 80 Daehak-ro, Buk-gu, Daegu 702-701, Korea*

<sup>b</sup>*Division of Advanced Nuclear Engineering, Pohang University of Science and Technology, San 31, Hyoja-dong, Nam-gu, Pohang 790-784, Korea*

<sup>c</sup>*Pohang Accelerator Laboratory, Pohang University of Science and Technology, San 31, Hyoja-dong, Nam-gu, Pohang 790-784, Korea*

**Abstract.** We report on activities using a pulsed neutron facility consisting of an electron linear accelerator, a water-cooled Ta target with a water moderator, and a 12 m time-of-flight path. It is possible to measure neutron total cross sections in the neutron energy range from 0.01 eV to a few hundred eV by using the neutron time-of-flight method; photo-neutron cross sections can also measure by using the bremsstrahlung from the electron linac. A <sup>6</sup>LiZnS(Ag) glass scintillator was used as a neutron detector. The neutron flight path from the water-cooled Ta target to the neutron detector was 12.1 m. In this paper, we report total cross sections of Nb and also resonance parameters obtained using the SAMMY fitting program. The present results are compared with the previous experimental results and the evaluated data in ENDF/B-VII. We also report on the mass-yield distribution of fission products in the 2.5-GeV bremsstrahlung-induced fission of <sup>nat</sup>Pb and <sup>209</sup>Bi measured at the 2.5-GeV electron linac using a recoil catcher and an off-line  $\gamma$ -ray spectrometric technique.

**Keywords:** Pulsed neutron facility, Time-of-flight method, Neutron total cross-section, Photo-neutron cross section, mass-yield distribution.

**PACS:** 29.87.+g, 25.60.Dz, 28.20.Ka, 29.20.Ej.

## INTRODUCTION

Electron linear accelerators (linac) are being used throughout the world in a variety of important applications. The pulsed neutron facility based on an electron linac is effective for measuring energy dependent cross sections with high resolution by the time-of-flight (TOF) technique covering the energy range from thermal neutrons to a few tens of MeV. The measurement of neutron cross sections gives basic information about the internal structure of atomic nuclei and their constituents. Precise measurements of neutron cross sections are of great importance for the safety design of nuclear reactors and for the evaluation of the neutron flux density and the energy spectrum around a reactor.

The pulsed neutron facility based on a 100-MeV electron linac was proposed in 1997 and construction was completed at the Pohang Accelerator Laboratory in 1999 [1]. Its main goal is to provide the infrastructure for nuclear data measurements in Korea.

## PULSED NEUTRON FACILITY

The pulsed neutron facility consists of an electron linac, a water-cooled Ta target, and a ~12-m-long TOF path. The characteristics of the facility are described elsewhere [2]. The beam energy of the electron linac is varied from 75 MeV to 50 MeV, and the beam currents at the end of linac are in between 100 mA and 30 mA. The length of electron beam pulse is 1-2  $\mu\text{s}$ , and the pulse repetition rate is 10 Hz. Pulsed neutrons were produced via the  $^{181}\text{Ta}(\gamma, xn)$  reaction by bombarding a metallic Ta-target with the pulsed electron beam. The estimated neutron yield per kW of beam power is  $1.9 \times 10^{12}$  n/s for electron energies above 50 MeV at the Ta-target based on the MCNP code [3]. To maximize the thermal neutrons in this facility, we used a cylindrical water moderator contained in an aluminum cylinder with a wall thickness of 0.5 cm, a diameter of 30 cm, and a height of 30 cm. The water level in this experiment was 3 cm above the target surface. The pulsed neutron beam was collimated to 5-cm diameter in the middle position of the collimation system where the sample changer was located. The sample changer consisted of a disc with 4 holes; each hole was 8-cm in diameter, which matched the hole in the collimator in the neutron beam line. The sample changer was controlled remotely by using a CAMAC module.

The neutron guide tubes were constructed of stainless steel with two different diameters, 15 cm and 20 cm, and were placed perpendicularly to the electron beam. The neutron collimation system was mainly composed of  $\text{H}_3\text{BO}_3$ , Pb, and Fe collimators, which were symmetrically tapered from a 10-cm diameter at the beginning to a 5-cm in the middle position where the sample was located, to an 8-cm diameter at the end of guide tube where the neutron detector was placed. There was a 1.8-m-thick concrete wall between the target and the detector room.

## NEUTRON TOTAL CROSS SECTION MEASUREMENT

Since the experimental procedure has been published previously [4-6], only a general description is given here. The experimental arrangement for the transmission measurements is shown in Fig. 1.

The neutron detector was located at a distance of 12.1 m from the photo-neutron target. A  $^6\text{Li-ZnS}(\text{Ag})$  scintillator (BC702) with a diameter of 12.5 cm and a thickness of 1.6 cm mounted on an EMI-93090 photomultiplier was used as a neutron detector. During the transmission measurement, the electron linac was operated with a repetition rate of 15 Hz, a pulse width of 1.1  $\mu\text{s}$ , and the electron energy of 65 MeV. The peak current in the beam current monitor located at the end of the second accelerator section was greater than 50 mA, which was almost the same as that in the target. A high purity (99.99%) natural niobium ( $^{93}\text{Nb}$  100% abundance in nature) metal plate with a diameter of  $80.11 \pm 0.01$  mm and thickness of  $15.04 \pm 0.03$  mm was used as a transmission sample. The main impurities of this sample were Ta (<0.1%), O (<0.06%), N (<0.04%), and C (<0.02%). A set of notch filters of Co, In, and Cd plates was used for the background measurement and the energy calibration. The configuration of the data acquisition system used in this measurement is also shown in Fig. 1, and details of this are described elsewhere [4].

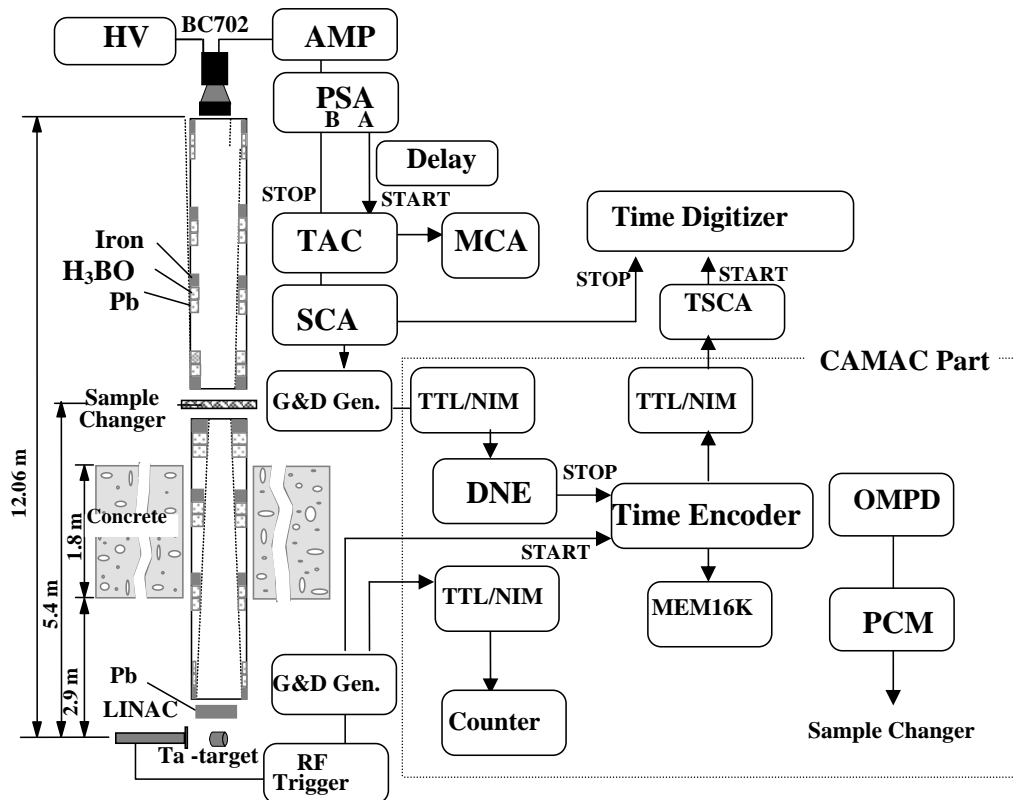


FIGURE 1. Configuration of experimental setup and data acquisition system.

The neutron total cross section is determined by measuring the transmitted neutrons through a known amount of sample and comparing this with the transmitted neutrons without sample. The accumulated neutron TOF spectrum for the open beam operation and for the transmission spectra of the natural Nb sample are shown in Fig. 2, together with the estimated background level, which is indicated by a solid line.

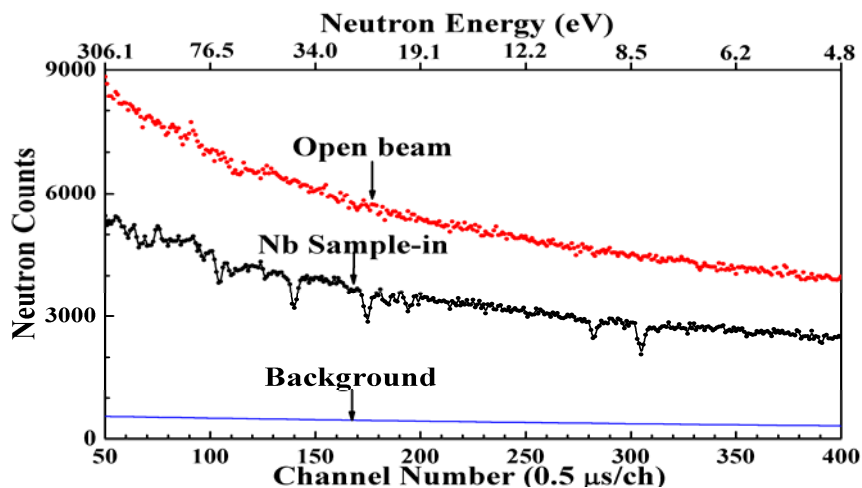
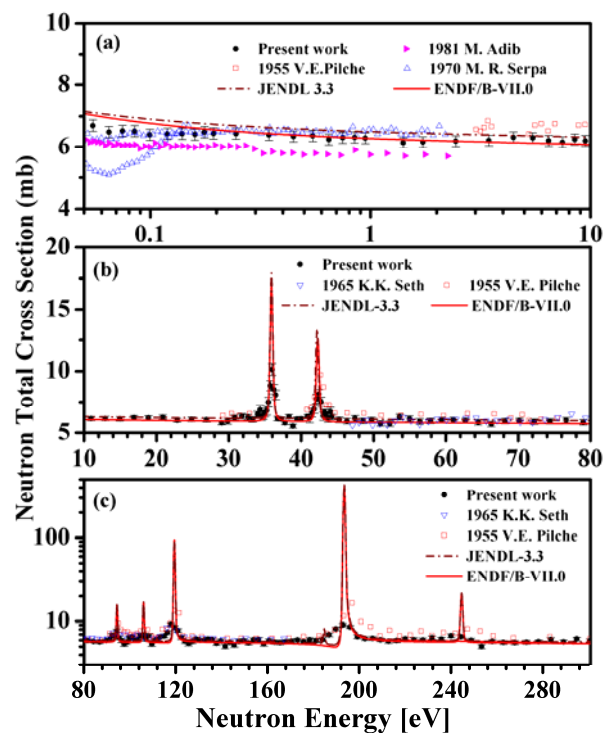


FIGURE 2. Neutron TOF spectra for the sample-in and for the sample out of 15-mm Nb, together with the estimated background level indicated as a solid line.

The total neutron cross sections for natural Nb were obtained in the neutron energy range from 0.05 to 300 eV assuming that numbers of count in each energy group are uniformly distributed. The overall statistical errors for the measured total cross sections ranged from 5% to 25%, depending on the neutron energy. The systematic uncertainties came from the following sources: uncertainties from the flight-path measurements (2.0%), the background estimation (0.04%), the sample thickness (2.6%), and the dead time, the normalization, etc. (2.0%). Thus, the total systematic error of the present measurement is about 3.8%.

The measured total cross sections are generally in good agreement with other existing data [7-10] and with ENDF/B-VII.0 [11] and JENDL 3.3 [12] evaluated data assuming 300 K for Doppler broadening, as shown in Fig. 3.



**FIGURE 3.** Measured total neutron cross sections for  $^{nat}\text{Nb}$  compared with previous experimental and evaluated data.

The data measured by M. Adib et al. [7] in the energy region from 0.00232 to 2.2461 eV are lower than present results. The data from M. R. Serpa [8] are almost similar to that of the present values in the energy region from 0.14 to 2.1 eV, but his results in the neutron energy below 0.14 eV are different from the present results and other measurements. The data measured by V. E. Pilcher et al. [9] are higher than the present results at energies from 3.03 to 9.47 eV and 29.2 to 299.7 eV, respectively.

K. K. Seth et al. [10] measured the total cross sections from 47.1 to 166.9 eV and their results are in general good agreement with the present results. The present results are in general good agreement with the evaluated data from ENDF/B-VII.0 [11] but slightly lower than those of JENDL 3.3 [12].

We fitted the transmission of the natural Nb sample with the SAMMY code [13] to obtain resonance parameters of each resonance peak in the neutron energy region from 10 to 280 eV, as shown in the Fig. 4.

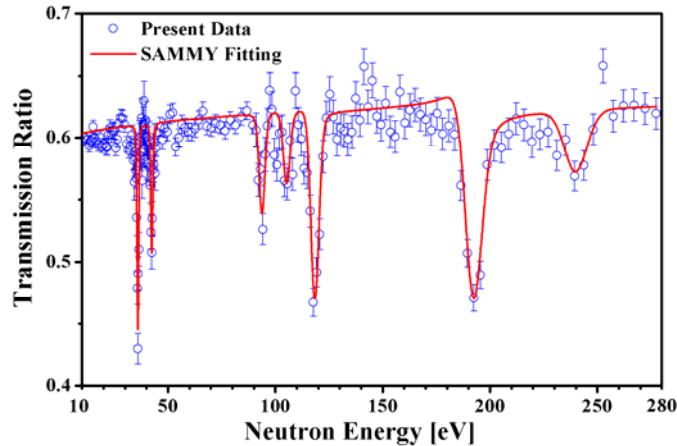


FIGURE 4. Measured transmission of Nb was fitted with the SAMMY code.

## MASS-YIELD DISTRIBUTION OF FISSION PRODUCTS

The mass-yield distribution of fission products in the 2.5-GeV bremsstrahlung-induced fission of  $^{nat}\text{Pb}$  and  $^{209}\text{Bi}$  has been measured by using a recoil catcher and an off-line  $\gamma$ -ray spectrometric technique. The experiment was carried out at the  $10^\circ$  beam line of the 2.5 GeV electron linac of the PAL. The details on the experiment are given elsewhere [14,15]. The bremsstrahlung was produced when a pulsed electron beam hit a tungsten (W) target with a size of  $5\text{ cm} \times 5\text{ cm}$  and a thickness of 1 mm. The W target was located at 38.5 cm from the electron exit window. The  $^{nat}\text{Pb}$  metal foil of 0.5 mm thick and  $25\text{ cm}^2$  area (12.417 g) and the  $^{209}\text{Bi}$  metal foil of 3 mm thick and  $25\text{ cm}^2$  area (74.417 g) were wrapped with 0.025 mm thick aluminum foil with purity more than 99.99%. Each sample was fixed on a stand in air at 24 cm from the W target and positioned at  $0^\circ$  with respect to the direction of the electron beam. Each sample was irradiated for 4-7 hours with the end point energy of 2.5-GeV bremsstrahlung. The irradiated target assembly was cooled for 2 hours. The aluminum catcher and the lead or the bismuth foil were taken out from the irradiated assembly and were mounted separately on two different Perspex (acrylic glass, 1.5 mm thick) plates. The Perspex plate with an Al catcher contains primarily fission products together with reaction products from the Al catcher itself. The other Perspex plate with an irradiated Pb (Bi) metal foil contains fission products and significant  $(\gamma, xn)$  reaction products from the lead (bismuth) foil with high  $\gamma$ -ray intensity.

The  $\gamma$ -ray activities from fission and reaction products were measured using an energy- and efficiency-calibrated HPGe detector coupled to a PC-based 4K-channel analyzer. The HPGe detector with 20% efficiency was a p-type coaxial CANBERRA detector of 7.62 cm diameter  $\times$  7.62 cm length. The  $\gamma$ -ray spectrum was obtained by using a program Gamma Vision 5.0 (EG&G Ortec).

The data analysis was done primarily from the  $\gamma$ -ray spectrum of the fission products of the Al catcher to avoid difficulties of efficiency calibration for low energy  $\gamma$ -rays in the thick lead or bismuth foil. The details on the data analysis are given elsewhere [14,15]. The absolute cumulative yields of the various fission products as a function of the mass number for the 2.5-GeV bremsstrahlung-induced fission of  $^{nat}\text{Pb}$  and  $^{209}\text{Bi}$  are plotted in Fig. 5. We do not consider the charge distribution corrections on the cumulative yields because of the closeness of the fission products to the beta stability line. The yields of fission products are fitted with a Gaussian curve to obtain the mean mass and the FWHM of the mass-yield distribution. The mean mass and the FWHM of the mass-yield distribution for the photo-fission of  $^{nat}\text{Pb}$  and  $^{209}\text{Bi}$  at 2.5-GeV bremsstrahlung are  $94\pm 0.5$  and  $55.0\pm 2.0$  mass units, and  $95.0\pm 0.5$  and  $51.0\pm 2.0$  mass units, respectively. The mean mass and the FWHM of the mass-yield distribution in the bremsstrahlung-induced fission of  $^{nat}\text{Pb}$  and  $^{209}\text{Bi}$  at various energies are given in Table 1 and also plotted in Fig. 6. It can be seen from Fig. 6 that for both  $^{nat}\text{Pb}$  and  $^{209}\text{Bi}$ , the FWHM of the mass-yield distribution increases with increasing bremsstrahlung energy. On the other hand, the mean mass of the mass-yield distribution decreases with increasing bremsstrahlung energy. These phenomena are due to the increase of the multi-nucleon emission and due to the increase of the multi-nucleon emission and the multi-chance of fission probability with increasing excitation energy.

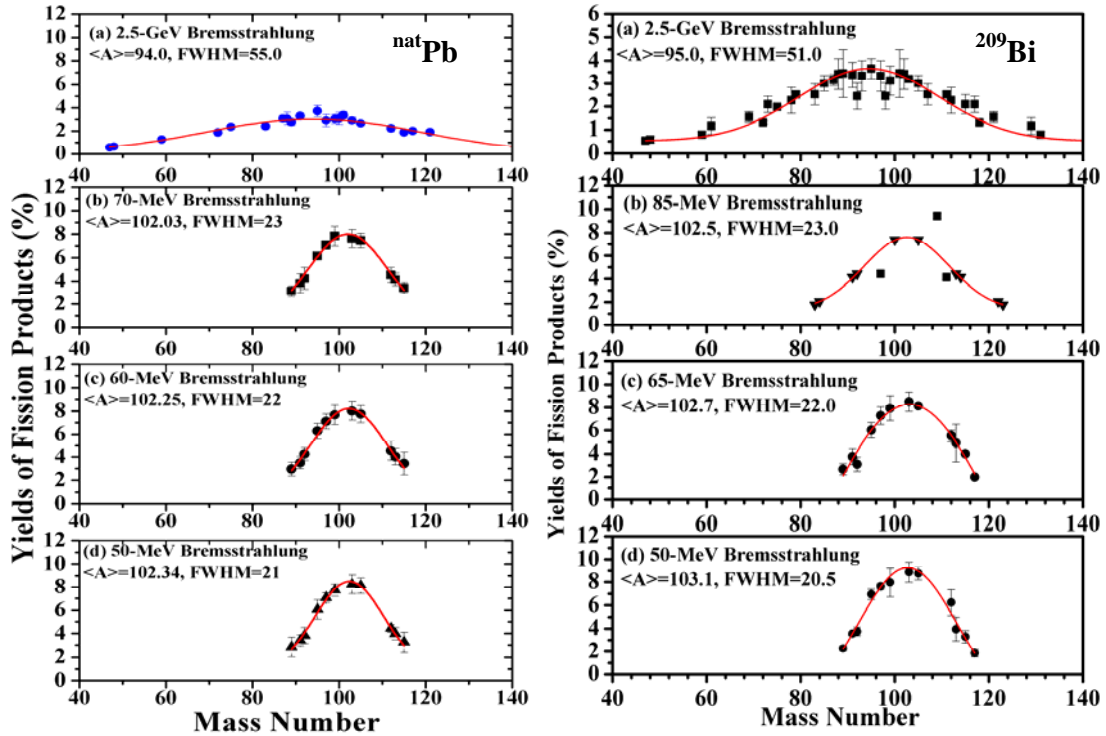


**FIGURE 5.** Measured yields of fission products (%) from the photo-fission of  $^{nat}\text{Pb}$  and  $^{209}\text{Bi}$  as a function of the mass number. The line indicates the fitting for the measured data points  $\langle A \rangle$  and FWHM are the mean mass number and the full-width at half-maximum of the mass-yield distribution.

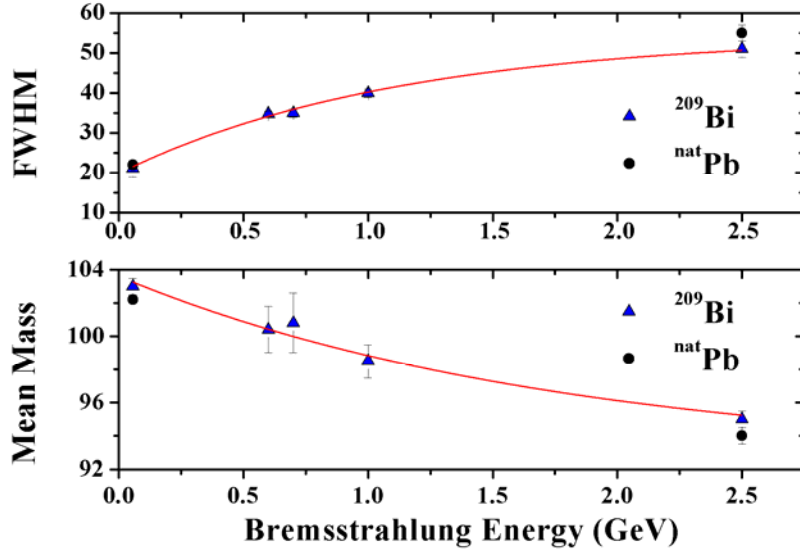


**FIGURE 6.** The FWHM and the mean mass of the mass-yield distributions for the photo-fission of  $^{\text{nat}}\text{Pb}$  and  $^{209}\text{Bi}$  as a function of the bremsstrahlung energy. The line indicates the polynomial fitting for the data points listed in Table 1.

**TABLE 1.** Mean mass and FWHM of the mass-yield distribution in the bremsstrahlung-induced fission of  $^{\text{nat}}\text{Pb}$  and  $^{209}\text{Bi}$ .

| Nuclei                   | Bremsstrahlung energy (MeV) | Mean mass (mass units) | FWHM (mass units) | References |
|--------------------------|-----------------------------|------------------------|-------------------|------------|
| $^{\text{nat}}\text{Pb}$ | 50                          | 102.34                 | 21                |            |
|                          | 60                          | 102.25                 | 22                |            |
|                          | 70                          | 102.03                 | 23                |            |
| $^{209}\text{Bi}$        | 2500                        | 94.0±0.5               | 55.0±2.0          |            |
|                          | 28-40                       | 103.5                  | 19.0              | [16]       |
|                          | 50                          | 103.1                  | 20.5              |            |
|                          | 65                          | 102.7                  | 22.0              |            |
|                          | 85                          | 102.5                  | 23.0              | [17]       |
|                          | 600                         | 100.4±1.4              | 34.8±0.7          | [18]       |
|                          | 700                         | 100.8±1.8              | 35.0±1.0          | [19]       |
|                          | 1000                        | 98.5±1.0               | 40.0±1.0          | [20]       |
|                          | 25000                       | 95.0±0.5               | 51.0±2.0          |            |

## DISCUSSION AND SUMMARY

The Pohang pulsed neutron facility based on an electron linac was constructed for nuclear data measurements in Korea. This paper has presented neutron total cross-sections and resonance parameters for  $^{\text{nat}}\text{Nb}$  in the neutron energy region from 0.01 eV to 300 eV. These cross sections and resonance parameters are in general consistent with other measured results and the evaluated data. We have also presented the mass-yield distributions of fission products of  $^{\text{nat}}\text{Pb}$  and  $^{209}\text{Bi}$  with bremsstrahlung energies of 50-70 MeV and 2.5 GeV. It was found that the mean mass of the mass yield distribution of the fission products decreases with the increasing bremsstrahlung energy. However, the FWHM of the mass yield distribution increases with the increasing bremsstrahlung energy.

## ACKNOWLEDGMENTS

The authors would like to express their sincere thanks to the staff of the Pohang Accelerator Laboratory for the excellent operation of the electron linac and their strong support. This work was partly supported by the National Research Foundation of Korea (NRF) through a grant provided by the Korean Ministry of Education, Science and Technology (MEST) in 2011 (Project No. 2011-0025762, 2011-0006306), by the World Class University (WCU) program (R31-30005), and by the Institutional Activity Program of Korea Atomic Research Institute.

## REFERENCES

1. G. N. Kim et al., *J. Korean Phys. Soc.* **38** (1), 14-18 (2001).
2. G. N. Kim et al., *Nucl. Instr. Meth. A* **485**, 458-467 (2002).
3. V. D. Nguyen et al., *J. Korean Phys. Soc.* **48** (3), 382-389 (2006).
4. V. Skoy et al., *J. Korean Phys. Soc.* **41** (3), 314-321 (2002).
5. A. Meaze et al., *J. Korean Phys. Soc.* **46** (2), 401-407 (2005).
6. T. Wang et al., *Nucl. Instr. Meth. B* **268** (2), 106-113 (2010).
7. M. Adib et al., <<http://www.nndc.bnl.gov/exfor7/exfor00.htm>>, EXFOR No. 30591.005 (1981).
8. M. R. Serpa, <<http://www.nndc.bnl.gov/exfor7/exfor00.htm>>, EXFOR No.10404.006 (1970).
9. V. E. Pilcher and R. L. Zimmerman, < <http://www.nndc.bnl.gov/exfor7/exfor00.htm>>, EXFOR No. 11909.002 (1955).
10. K. K. Seth, D. J. Hughes, R. L. Zimmerman, and R. C. Garth, *Phys. Rev.* **110** (3), 692-700 (1958).
11. M. B. Chadwick et al. *NuclearData Sheets* **107** (12), 2931-3060 (2006).
12. K. Shibata et al., *J. Nucl. Sci. Technol.* **39** (11), 1125-1136 (2002).
13. N. M. Larson, ORNL/TM-9179/R5, Oak Ridge National Laboratory (2000).
14. H. Naik et al., *Eur. Phys. J. A* **47**(3), 37- 46 (2011).
15. H. Naik et al., *Nucl. Instr. Meth. B* **267**(11), 1891-1898 (2009).
16. R.V. Warnock, R.C. Jensen, *J. Inorg. Nucl. Chem.* **30** (8), 2011-2016 (1968).
17. N. Sugarman, *Phys. Rev.* **79** (3), 532-533 (1950).
18. M. Areskoug, B. Schroder, K. Lindgren, *Nucl. Phys. A* **251** (3), 418-432 (1975).
19. B. Schroder, G. Nydahl, B. Forkman, *Nucl. Phys. A* **143** (3), 449-467 (1970).
20. A.P. Komar et al., *Sov. J. Nucl. Phys.* **10**, 30-35 (1970).